

**The Invariant Mass Spectra Profile
Close to Pentaquark Mass Region
at $1.54 \text{ GeV}/c^2$.**

M.Zavertyaev

Max-Planck Institut für Kernphysik, D-69117 Heidelberg, Germany
P.N.Lebedev Physical Institute, 117924 Moscow B-333, Russia

Abstract

Two possible reasons for the narrow peak observation in the invariant mass spectrum of the pK_s^0 close to $1.54 \text{ GeV}/c^2$ are discussed.

1 Introduction

Five different experiments have reported the observation of a narrow peak in the invariant mass spectra close to $1.54\text{GeV}/c^2$ with a width below $25\text{MeV}/c^2$. These peaks are considered as a signature of a five quark resonance, the so-called θ^+ .

Three photo-production experiments [1, 2, 3] have observed the θ^+ decay to nK^+ in three- or four- body final state. The neutron was reconstructed from the missing mass and energy.

The θ^+ decay to pK_s^0 was observed in $\nu_{\mu^-}(\bar{\nu}_{\mu^-})$ collisions with nuclei [4]. This analysis has combined data samples from different bubble chamber experiments with a large range of neutrino momenta.

Using a K^+ beam, the same pK_s^0 channel of the θ^+ decay was observed by the DIANA collaboration [5]. The Monte Carlo simulation for this experiment is rather simple for the following reason: first - the beam momentum spectrum is explicitly shown in the publication, second - all particles in the final state (p and $K_s^0 \rightarrow \pi^+\pi^-$) were reconstructed and identified.

The result of the simulation for the DIANA experiment are presented in the section below. One section further the result of the experiment “independent” simulation shows the possible source of the narrow peak in the invariant mass spectrum.

2 Monte Carlo simulation.

The experimental momentum spectrum of the incident beam particle K^+ (Fig. 1) is shown for two cases: the momentum spectrum for all events with the identified K_s^0 (top), and for events where both the K_s^0 and the proton were identified [5] (bottom). The momentum spectra look very different, both in momentum range and in shape. For the events with pK_s^0 in the final state the momentum profile has an asymmetric “bell”-like shape with the average momentum close to $470\text{MeV}/c$.

The K^+ momentum spectrum was simulated according to the experimental distribution shown in Fig. 1b. The momenta of the outgoing particles are generated uniformly in the available Lorentz-invariant phase space. Two processes are simulated :

- three body final state - a nucleus play a role of the recoil particle:
 $K^+Xe \rightarrow pK_s^0Xe'$
- two body final state - a charge-exchange reaction on the neutron of the Xe nucleus:
 $K^+n \rightarrow pK_s^0$
The momentum is shared by two particles only.

The pK_s^0 invariant mass spectrum for three body final state simulation is shown in Fig. 2b. The comparison with the experimental distribution (“red” histogram) shows a reasonable agreement in positions, widths and shapes of both spectra.

The invariant mass spectrum for the two body final state pK_s^0 is shown in Fig. 2c. In contrast to the three body final state pK_s^0Xe' the mass distribution resembles narrow peak with a sharp maximum at $1.55\text{GeV}/c^2$.

The simple MC test with the K^+ momentum spectrum of the gaussian shape (the mean at $450\text{MeV}/c$ and the width $15\text{MeV}/c$) shows that the narrow momentum range of the incident K^+ beam is the reason why the narrow peak is seen in the mass spectrum in case of two body final state (Fig. 3c). The shift of the K^+ momentum distribution by $20\text{MeV}/c$ gives the proportional shift by $10\text{MeV}/c^2$ in the mass peak position (Fig. 3d) and puts the maximum at $1.54\text{GeV}/c^2$.

The simulation of the pK_s^0 kinematic disagree with the observed invariant mass spectrum only in one point - peaks are shifted by $10\text{-}15\text{MeV}/c$. This shift may come from the fact that in the MC the binding energy of the nucleus was not included in the simulation. There is an explicit indication in reference [5] that the K^+ beam momentum was shifted by $\pm 15\text{MeV}/c$ in different data sample, but there is no indication about the corresponding statistics, accumulated with a particular beam momenta. As result, the MC events were not weighted and that may also cause some kind of shift in the peak position. The difference in the width is not too important -the MC shows that with statistic of about 30 event, the narrow peak may be observed even if the original distribution is wide (Fig. 4). The narrow two-bin peak distribution, when at least 50% of entries belongs to two bins only, was observed in 2% cases - a non-negligible number.

3 The kinematic “reflection” at $1.54\text{GeV}/c^2$.

Since the mass region around $1.54\text{GeV}/c^2$ has so much importance in the narrow peak search, another source of trouble must be pointed out.

In a data sample of V^0 candidates (V^0 is used as a generic name for K_s^0 , Λ or $\bar{\Lambda}$) the narrow peak in the mass spectrum may be created in the following way.

A V^0 decays in two particles of opposite charge. Since the type of the particle is not known in the experiment the different mass hypothesis have to be assigned to each track to explore all combinations. With pion and proton/anti-proton masses assigned to corresponding tracks, each V^0 may represent K_s^0 , Λ or $\bar{\Lambda}$.

The most convenient way to present the kinematic of the V^0 decays is an Armentero-Podolansky plot [6], shown in Fig. 5, where the three ellipses correspond to $K_s^0 \rightarrow \pi^+ \pi^-$, $\Lambda \rightarrow p \pi^-$ and $\bar{\Lambda} \rightarrow \bar{p} \pi^+$ decays. The ellipses have two overlap regions where this V^0 species are kinematically indistinguishable. Therefore, without an explicit cut on the corresponding mass hypothesis, there is always a cross contamination. For example K_s^0 may be not a “true” K_s^0 but a Λ or $\bar{\Lambda}$ in these narrow kinematic regions.

In second step the V^0 is then combined with the same physical track which was already used to for the V^0 itself. Two class of combination may be defined:

- True K_s^0 and the π^+ of the K_s^0 but considered as a proton (class 1).
- True Λ but considered as a K_s^0 and a positive track of the Λ which is a true proton (class 2).

Figures 6 and 7 show the invariant mass distributions for the two classes of combinations defined above.

The standard cut used in all experimental analysis is a cut on the invariant mass of the $\pi^+ \pi^-$ combination around K_s^0 mass ($|m_{K_s^0} \pm m_{\pi^+ \pi^-}| < 3 \cdot \sigma$). The usual mass resolution for two track combinations is limited to $\sigma=2-4\text{MeV}/c$. For class 1 this cut does not change the invariant mass distribution (true K_s^0), but for class 2 this cut removes combinations with small masses and retains combinations around $1.54\text{GeV}/c^2$ (Fig. 8). Fig. 9 shows the combined (class 1 and class 2) mass spectrum.

It is hardly believable that a straight forward double track counting may happen in a real analysis. At least for DIANA this possibility is excluded by the nature of the experiment - in the bubble chamber all tracks are visible. The problem might be important for the electronic experiment if the cut on V^0 masses is not tight enough, thus the K_s^0 - Λ cross contamination is not removed completely, and the pool of reconstructed tracks is not free from “clones” or “ghosts” - de-facto the same track reconstructed twice due to , for example, some noise in the tracking detectors. The kinematic of such “clones” is very close to each other thus simulating the situation discussed above, naturally with a slight variation in the mass position and the width of the peak.

4 Conclusion.

The result of the simple MC shows that the invariant mass spectrum of the pK_s^0 combinations has a narrow structure close to $1.54\text{GeV}/c^2$ due to the narrow momentum range of the beam. If this is true, then further data analysis using the full moment range of the beam (see Fig. 1a) will cause the broadening of the observed peak and yield the answer about its nature.

The artificial peaks in the invariant mass spectra due to kinematic reasons are well known. The only surprise is that such an artifact precisely coincides with the value of $1.54\text{GeV}/c^2$.

The recent publication [7] shows that the nK^+ channel is not free from the kinematic reflections.

Finally the question about the pentaquark signature will be found in a very classical way - increasing the statistic involved in the analysis and hopefully in a different experimental conditions.

Acknowledgments

The author acknowledge very useful discussions with J.Blouw, K.T.Knöpfle, M.Schmelling and B.Schwingerheuer.

References

- [1] T.Nakano *et al.*, *Evidence for a Narrow $S=+1$ Baryon resonance in photo-production from the Neutron*, Phys. Rev. Lett. **91** (2003) 012002-1.
- [2] S.Stepanyan *et al.*(CLAS collaboration), *Observation of on Exotic $S=+1$ Baryon in Exclusive Photoproduction from the Deuteron*, hep-ex/0307018 (16 Jul 2003).
- [3] J.Barth *et al.*(SAPHIR collaboration), *Evidence for the positive-strangeness pentaquark Θ^+ in photoproduction with the SAPHIR detector at ELSA*, hep-ex/0307083 (6 Aug 2003).
- [4] A.E.Asratyan, A.G.Dolgolenko and Kubantsev, *Evidence for the formation of a narrow pK_s^0 resonance with mass near 1533MeV in neutrino interactions*, hep-ex/0309042 (23 Sep 2003).
- [5] V.V.Barmin *et al.* (DIANA collaboration), *Observation of a baryon resonance with positive strangeness in K^+ collisions with Xe nuclei*, Yad. Phys **66** (2003) 1763-1766, or Phys. At. Nucl.**66** (2003) 1715-1718, hep-ex/0304040 (12 May 2003).
- [6] J.Podolansky and R.Armenteros, Phil.Mag. **45** (1954) 13.
- [7] A.R.Dziebra *et al.*, *The Evidence for a Pentaquark Signal and Kinematic Reflections*, hep-ex/0311125 (10 Nov 2003).

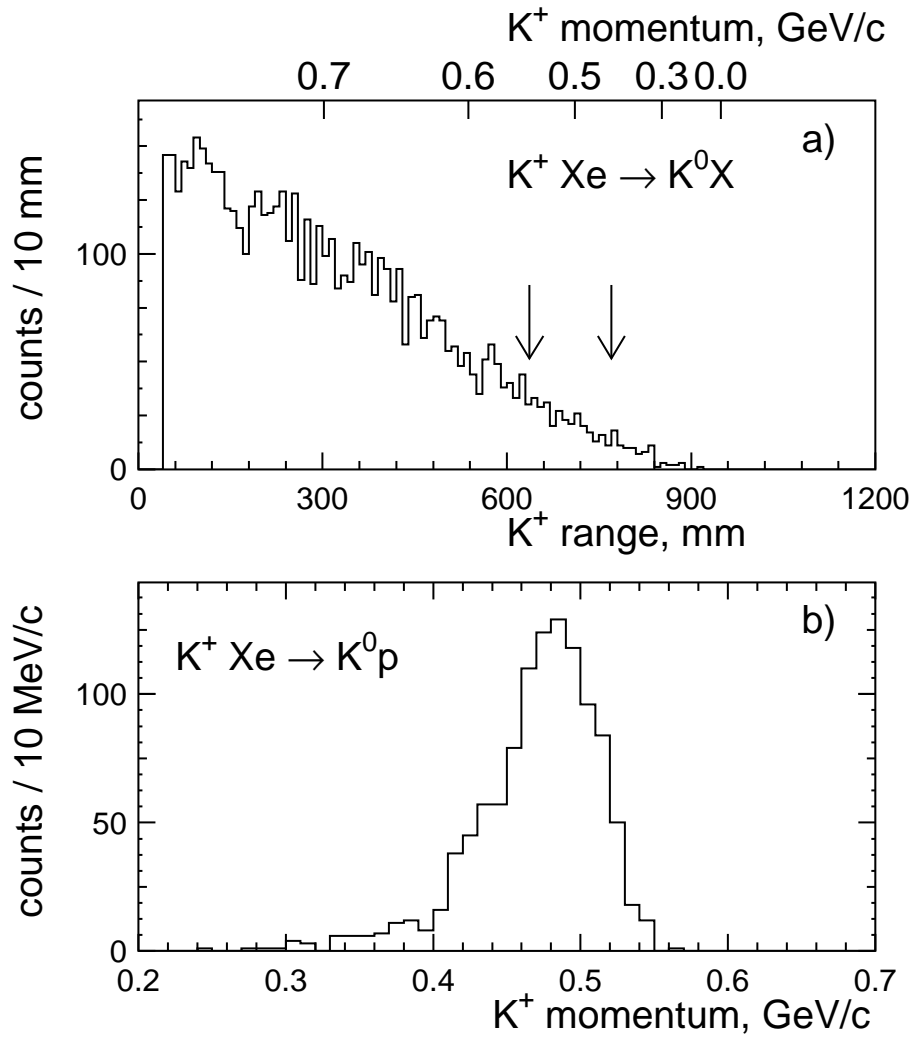


Figure 1: a) The range and equivalent momentum (upper scale) of the K^+ beam for the events with K_s^0 identification only. The arrows indicate the momentum region of the $p K_s^0$ selection. b) The momentum of the K^+ beam for the events with $p K_s^0$ identification. The momentum distributions were taken from [5]

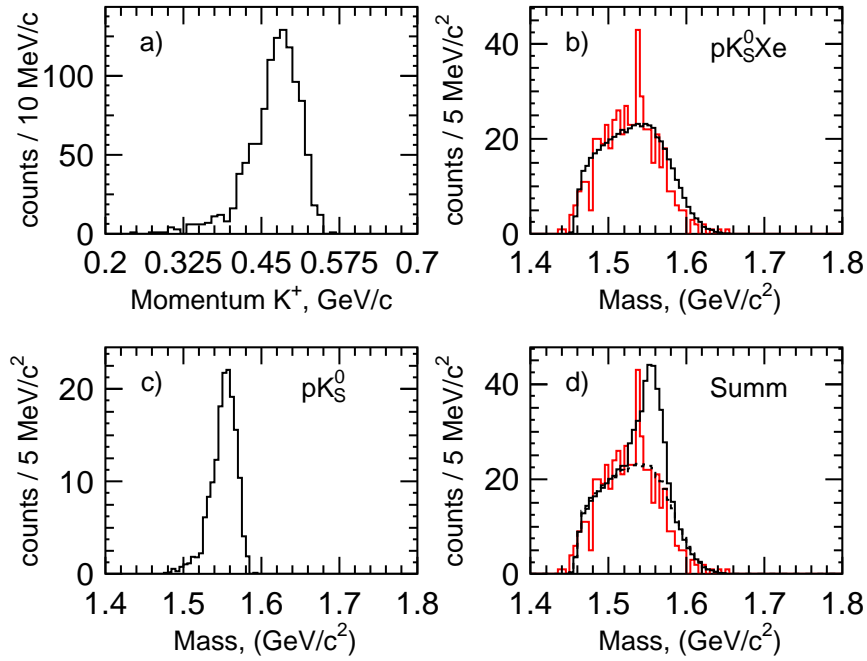


Figure 2: The experimental beam momentum [5] and MC mass spectra distribution corresponding to: b) reaction $K^+Xe \rightarrow K_s^0 p X e'$; c) reaction $K^+n \rightarrow K_s^0 p$; d) the summ of both b) and c); The histogram in red corresponds to the experimental mass distribution from [5].

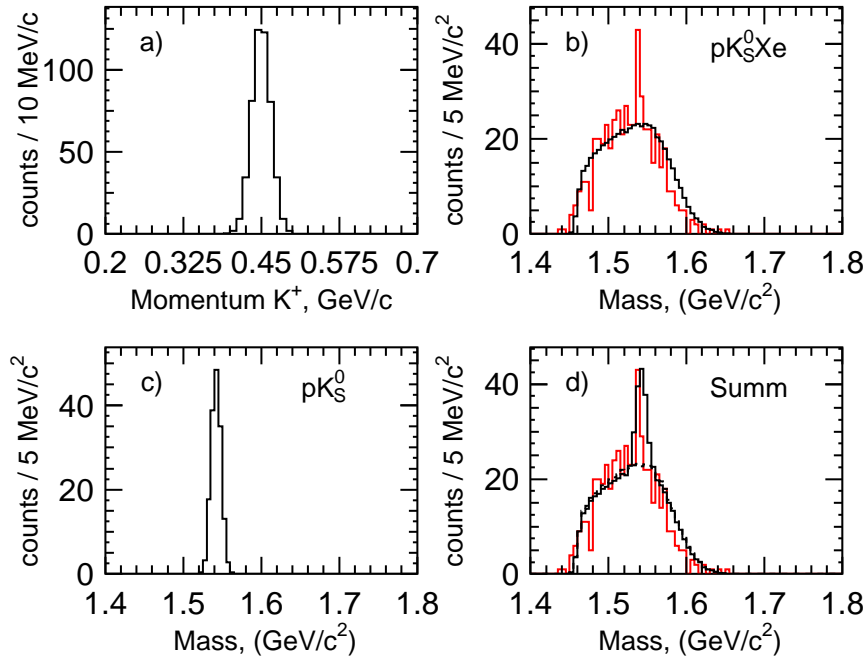


Figure 3: The beam momentum simulated according to the gaussian shape and MC mass spectra distribution corresponding to: b) reaction $K^+Xe \rightarrow K_S^0 p X e'$; c) reaction $K^+n \rightarrow K_S^0 p$; d) the summ of both b) and c); The histogram in red corresponds to the experimental mass distribution from [5].

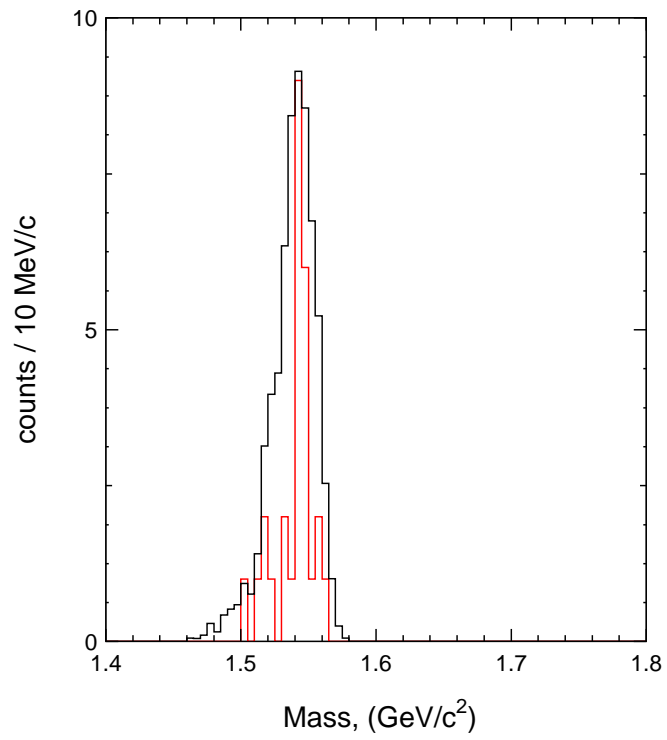


Figure 4: The invariant mass distribution for pK_s^0 combination in case, when at least 50% of entries were observed in two bins (red) and the “true” distribution shape (black) in case of big number of entries.

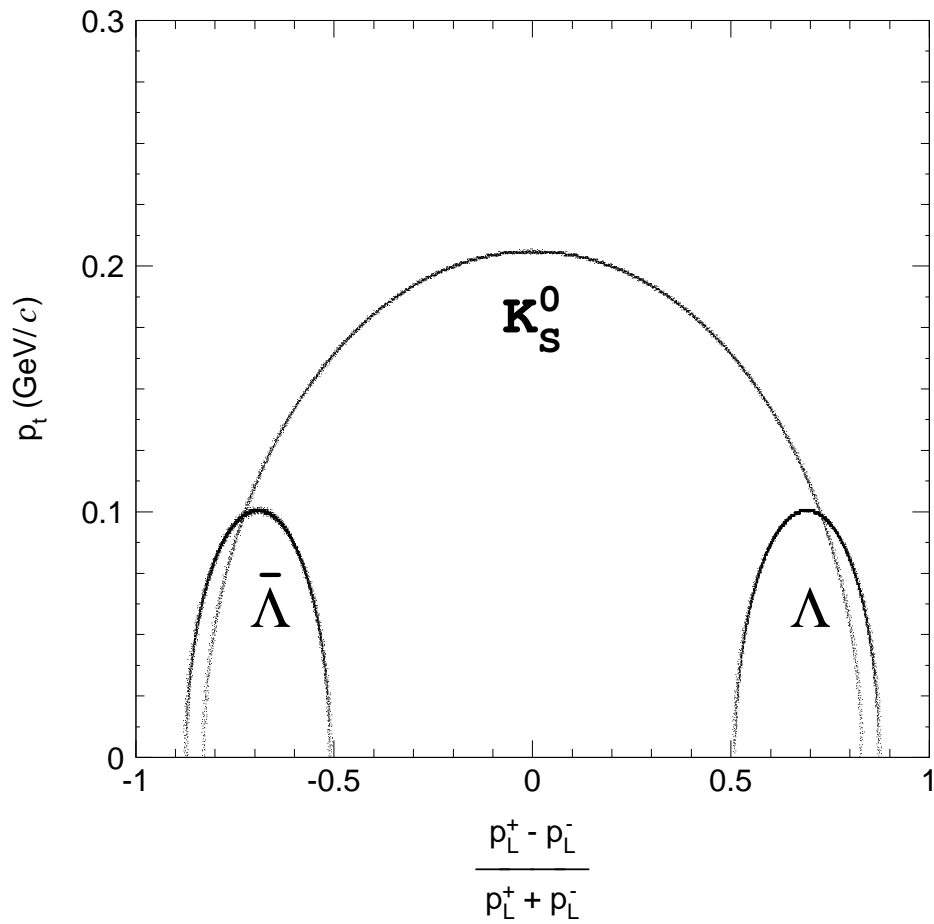


Figure 5: The Armenteros-Podolansky plot for the V^0 candidates. p_L^\pm and p_t are the laboratory longitudinal and transverse momenta, respectively, of the decay tracks with respect to the V^0 direction. At the crossing point of the two ellipses the K_S^0 and Λ kinematically looks the same.

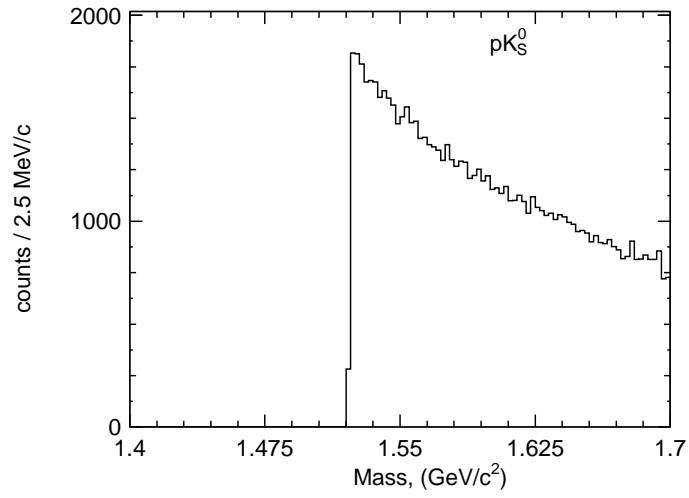


Figure 6: The invariant mass distribution for pK_s^0 combination of class 1.

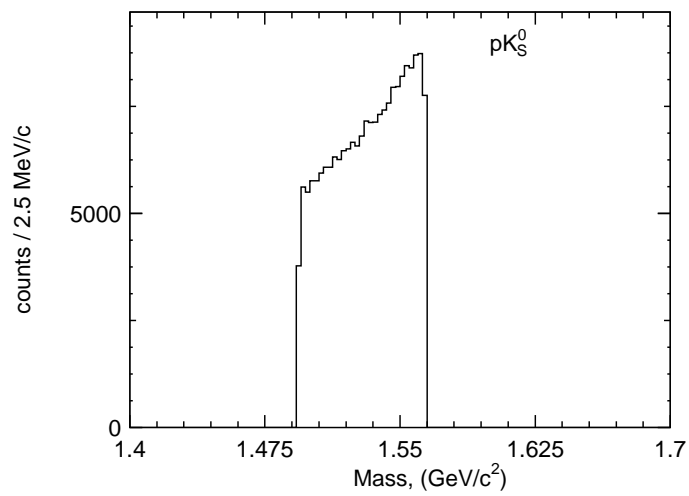


Figure 7: The invariant mass distribution for pK_s^0 combination of class 2.

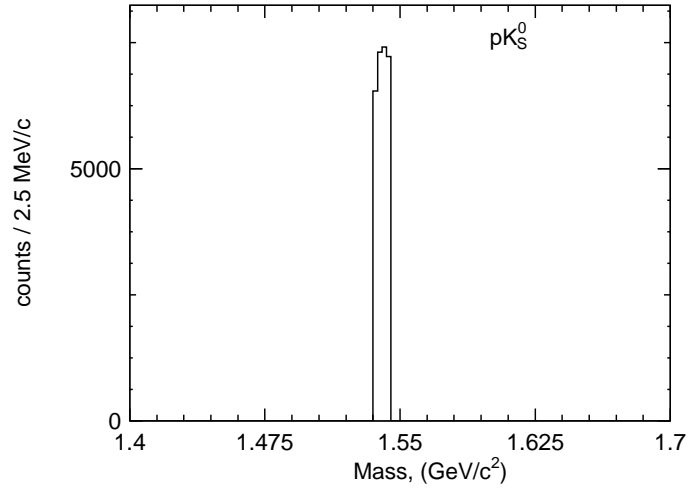


Figure 8: The invariant mass distribution for pK_s^0 combination of class 2 when the K_s^0 mass is limited within the K_s^0 mass region.

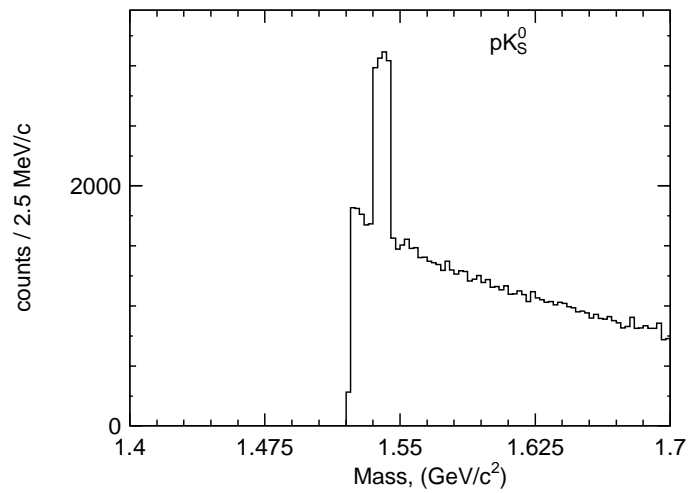


Figure 9: The combined invariant mass distribution for pK_s^0 combination of class 1 and class 2, when the K_s^0 mass is limited within the K_s^0 mass peak region.